

Influence of Graphite Content on Corrosion Behavior of Cartridge Brass in a 3.5 wt. % NaCl Solution

Mohammed Ali Almomani^{*}, Wail Radwan Tayfour, Mohammed Hani Nimrat

Industrial Engineering Department, Jordan University of Science and Technology, P. O. Box 3030, Irbid 22110, Jordan.

*E-mail: maalmomani7@just.edu.jo

Received: 22 October 2015 / Accepted: 6 January 2015 / Published: 4 May 2015

Several cartridge brass (Cu-30Zn) metal matrix composites reinforced with different weight fractions of graphite (Gr) particles were fabricated using the powder metallurgy (PM) method. Potentiodynamic testing was used to examine the corrosion behavior of both base monolithic alloy and composites in a simulated sea water solution (3.5 wt% NaCl solution). The results revealed that Cu-30Zn reinforced with active graphite particles shows a higher tendency to uniform corrosion as compared to the corresponding monolithic matrix alloy; due to the strong microgalvanic couple between conductive graphite particles and matrix material, and also the increase of cathodic area with increase of graphite weight fractions. The electrochemical results also shows the increase of efficiency of corrosion products layer after transpassive dissolution stage. This is due to the formation of crevice regions at the particle matrix interface which impede propagation of pits into the matrix. Both morphology and elemental analysis of the samples' surfaces before and after testing were examined using Scanning Electron Microscope (SEM) that is equipped with Energy Dispersive Spectroscopy (EDAX) system. The corroded surface of the composites is covered with the corrosion byproduct layer with large number of small shallow pits. This result is consistent with negative hysteresis attained at electrochemical testing.

Keywords: Uniform; Localized corrosion; Galvanic corrosion; Metal matrix composite; Cartridge brass; Graphite.

1. INTRODUCTION

The capability of controlling properties of metal matrix composites (MMC) by selecting the composite constituents phases (matrix and dispersed phase), processing methods spread out their uses for a wide variety of applications [1,2]. Copper based alloys are among the most commonly used alloys in heat exchangers, and cooling systems, as they own good thermal properties, and resistance

against corrosion [3,4]. One of the most commonly used copper alloys is brass that is made by adding a controlled amount of zinc to the base copper, where the variation of zinc content in the brass determines the properties of the produced alloy, and thus its applications [5,6].

Casting and powder metallurgy (PM) are widely used to produce MMCs. Hard control of second phase distribution and its accumulation in the molten metal matrix, with the possibility of reaction occurrence at matrix - reinforcing particles retard the use of casting in some cases [7,8]. On the other hand, it is easy to avoid these limitations to an acceptable limit using powder metallurgy route. Consequently, powder metallurgy offers a replacement to casting in these cases, especially its able to produce net shape products with a minimal need of secondary operations, and thus, at relatively low cost [9]. Even though these advantages of PM, its' products are porous with poor mechanical strength. Therefore, improving mechanical properties of PM products attracts the interest of many researchers who developed various techniques to control porosities of compact product as shot peening which was used to improve compressive strength of Fe/Cu -graphite composites [10].

The outstanding qualities of copper matrix composites with good attractive capabilities of powder metallurgy together inspire the future for new uses for these materials. Therefore, copper based composites reinforced with either single or two types of ceramic particles, i.e., SiC, Al₂O₃ are being produced [11].

Over the years, an extensive research effort has been carried out to develop materials with a good combination of high electrical conductivity, and good mechanical properties especially for high operating temperature applications. The possibility of developing strong and conductive brass has received too much attention of scholars who attempts to increase strength of brass and still retaining high conductivity. In the available literature, most work focus on incorporating some metallic alloying elements to the brass Cu-40Zn to utilize advantage of potential occurrence of precipitation hardening, or grain refinement. Powder metallurgy was the processing route in these research studies. For example, titanium addition improves mechanical properties of Cu-40Zn due to precipitation hardening [12]. Adding tin to Cu-40Zn-Ti alloy enhances mechanical properties by refining the grain [13]. Similar results attained upon introducing magnesium particles to Cu-40Zn brass alloy which effectively hinder the grain growth, and improve alloy strength [14].

Cu-30Zn brass alloy has many attractive properties including: good formability, good strength, and high corrosion resistance. It is used in making wide variety of products as flashlight shells, ammunition cases, heat exchangers, radiators,..etc [6]. Some of these products are used in a very aggressive corrosive environments. The precision of dimensional and geometrical tolerances is a requirement for many of these products. Hence, machinability is a key factor that determines the use of this alloy with a satisfactory finish at low cost. Lead was used widely in MMCs to improve its machinability. The low cost of graphite, non toxicity, and its ability to improve machinability encourage the use of graphite as a replacement material of lead in MMCs [15]. Therefore, it is important to examine the corrosion behavior of Cu-30Zn alloy in a simulated marine environments using 3.5 wt. % NaCl solutions, especially that there is no work or little work has published in the literature on this brass composite.

2. EXPERIMENTAL PROCEDURE

Powder metallurgy was used to produce Cu-30Zn alloy, and Cu-30Zn matrix reinforced with different weight fractions (0.1, 0.3, and 0.5) of graphite particles. Cu-30Zn was in the form of milled alloyed powder, and both types of used particles was less than 100 Mesh (149 microns) in size. Table 1 shows the producer and characteristics of each one of the used powders. The constituent particles were weighed precisely, and then shaken to disperse graphite particles homogenously in the matrix powder. 500 MPa was applied using universal testing machine to press the powder mixture in a high carbon steel die, shown in figure 1. Then, the green compact was backed at 650 °C for an hour.

Table 1. The examined powders producers/suppliers and characteristics

Powder	Producer/ Supplier	Powder characteristics
Alloyed Cu-30Zn	Zhejiang Jililai New Material Co., Ltd.	Mesh \leq 100 Water atomized Irregular shape particles.
Graphite	Chemsavers	Fine milled coal. Mesh \leq 100

The sintered sample was mounted onto bakelite puck in order to leave only one uncovered surface. To examine corrosion behavior, the sample was used as a working electrode in the corrosion cell, graphite and calomel was used as counter and reference electrodes, respectively. The exposed surface was polished with 1000 grit size emery paper, and 3.5 wt. % NaCl solution was used as electrolyte.

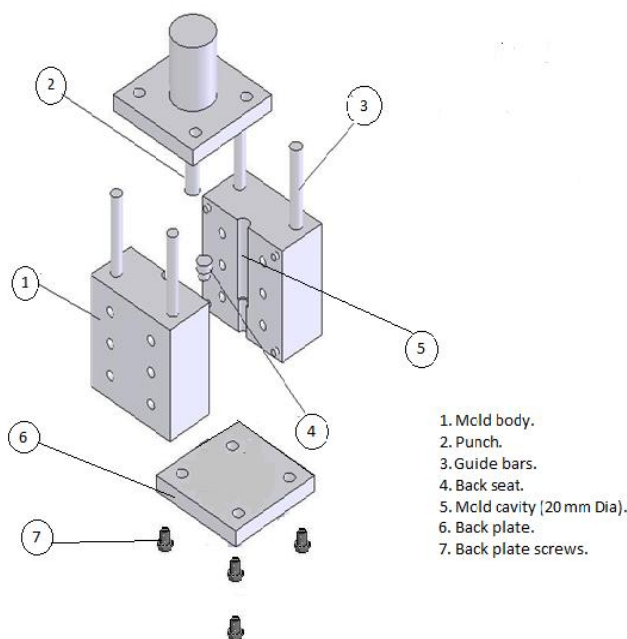


Figure 1. An exploded 3D model of the first compaction die.

Gamry potentiostat reference 600 was used to conduct polarization experiments for the examined alloy and composites. The potential was varied at scan rate of 0.1667 mV/sec from (-250 to 1000) and then back to -250 mV versus open circuit potential (OCP). SEM was used to examine the surface morphology of the samples prior and post corrosion testing. Elemental analysis of the intact surface and corroded surface was conducted using EDS. To determine the corrosion rates of the produced Cu-30Zn alloy, and Cu-30Zn matrix reinforced with graphite particles, Tafel extrapolation procedure was applied on the obtained polarization curves using Gamry Electrochemist Analyst software by intersecting the extension of linear segments or tangent lines of anodic and cathodic branches of the polarization curves.

3. RESULTS AND DISCUSSION

3.1 Polarization Measurement

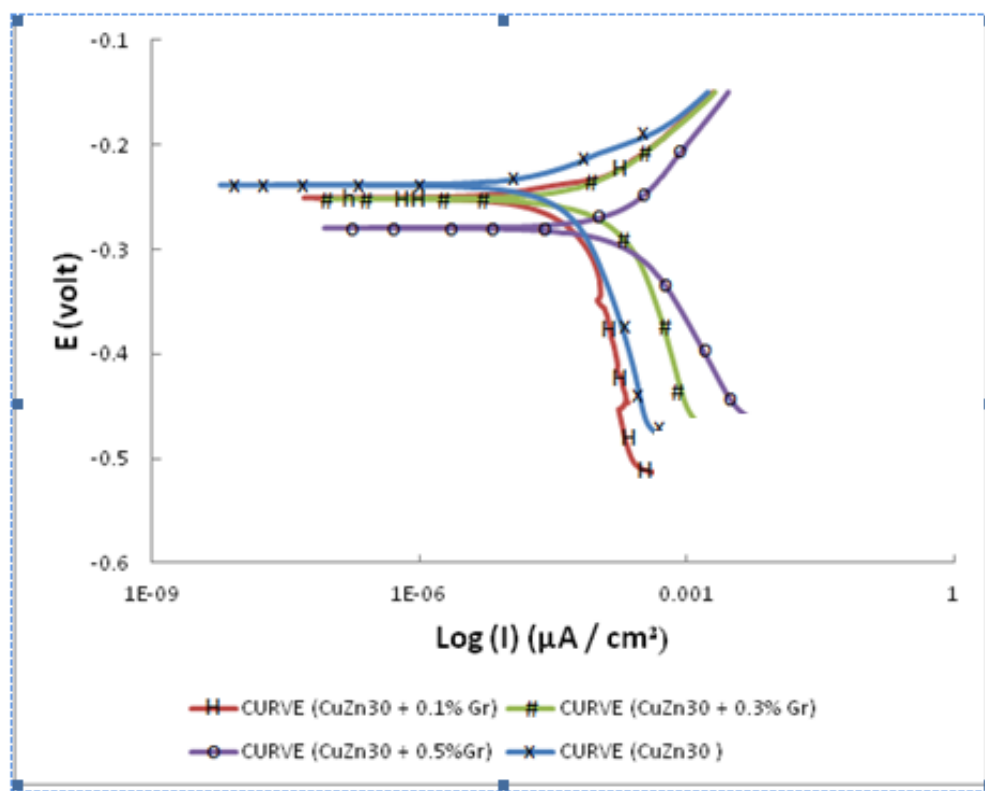


Figure 2. Tafel plots of the Cu-30Zn reinforced with different weight percentages of graphite in 3.5% NaCl solution.

The results show that the corrosion rate for Cu-30Zn reinforced with graphite is higher than the corrosion rate of the corresponding monolithic matrix alloy. Table 2 shows how a weight fraction of graphite will impact corrosion parameters of the produced composites, and presents the corrosion parameters of Cu-30Zn reinforced by graphite, as extracted from the Tafel region of the corresponding polarization curves. The results illustrate that adding graphite shifts the corrosion potential to values

more negative than E_{corr} obtained from monolithic alloy. Corrosion current densities increase, and also corrosion rates increase. Anodic and cathodic Tafel slopes are also influenced by the weight fraction of graphite reinforcement. The values of the cathodic Tafel slopes were decreased after adding graphite, which indicates that kinetics of hydrogen evolution is influenced by graphite content. Also, the values of the anodic Tafel slopes were increased only to small extent. This indicates that the change of potential causes a smaller rate of current change during anodic polarization than that during cathodic polarization. Figure 2 shows the Tafel regions of Cu-30Zn reinforced with different weight fractions of graphite.

Table 2. The corrosion parameters of Cu-30Zn reinforced with different weight fractions of graphite in 3.5 wt.% NaCl solution.

Material	Corrosion potential E_{corr} (mV vs. SCE)	Corrosion current, I_{corr} , ($\mu\text{A}/\text{cm}^2$)	Corrosion rate (mpy)	Anodic slope, β_a , (mV/decade)	Cathodic slope, β_c , (mV/decade)
Cu-30Zn	-238	4.99	0.3029	23.8	38.8
Cu-30Zn+0.1 wt% G	-251	20.9	1.278	30.9	90.3
Cu-30Zn+0.3 wt% G	-252	32.9	2.016	35.7	42.4
Cu-30Zn+0.5 wt% G	-279	38.4	2.350	46.1	32.2

The retardation of the corrosion resistance of the composite with the increase of weight fraction of graphite reinforcing particles can be attributed to: (1) the formation of strong microgalvanic couple between matrix and conductive graphite reinforcement particle, (2) the increase of cathodic area as the weight fraction of graphite increases, so the reduction current has more surface to occur, which causes an increase in the anodic dissolution rate, and thus the corrosion rate increased. Similar results were observed for other metal graphite composites; i.e. aluminum graphite composite [16,17], zinc graphite composite [18], copper graphite composite [19]. In these studies, it was found that introducing graphite particles has a negative effect on the corrosion resistance of pure metal as a result of formation strong galvanic couple between conductive graphite reinforcement particles, and conductive metal matrix, also the corrosion resistance of metal/graphite MMC decreased with the increase of graphite weight percentages. Furthermore, incorporating graphite fibers into metal matrix reduces corrosion resistance of metal matrix with increase of graphite-metal surface area ratio [20,21].

The polarization curves of the base alloy and examined composites follow a generic shape, as the one shown in figure 3. The curve provides a sign to surface passivation. Such passive layer was reported previously in the literature, as a complex mixture of CuO , Cu_2O , ZnO , $\text{Cu}(\text{OH})_2$, $\text{Cu}_2\text{Cl}(\text{OH})_3$, $\text{Zn}(\text{OH})_8$ $\text{Cl}_2\text{H}_2\text{O}$ [3,4,22,23]. Also, a stable protective passive layer $\text{Al}(\text{OH})_3$ was observed in $\text{Al5083-Al}_2\text{O}_3\text{-Gr}$ hybrid composites [24]. Table 3 summarizes the localized corrosion parameters of Cu-30Zn reinforced by different weight fractions of graphite. The curve shows that a reduction in the stability of the film with the increase of weight fraction of the enforcements due to heterogeneity of the corrosion product layer, and its' discontinuity at the particle matrix interface [25,26]. This conclusion is based on the reduction of passivation-depassivation current interval, as given by $\Delta I = I_{\text{crit}} - I_{\text{dep}}$. The electrochemical results also shows the increase of efficiency of corrosion product layer after

transpassive dissolution stage as the difference between passivation potential and free corrosion potential, ΔE , gets larger with increase of weight fraction of graphite [27]. This is due to the formation of crevice regions at the particle matrix interface which impede propagation of pits into the matrix [28].

Table 3. Localized Corrosion parameters of Cu-30Zn reinforced with different weight fractions of graphite

Material	ΔI (mA)	E_{corr} (mV vs SCE)	E_{rep} (mV vs SCE)	ΔE (mV)
Cu-30Zn	18.81	-235	-158	77
Cu-30Zn + 0.1 wt. % Gr	17.25	-250	-171	79
Cu-30Zn + 0.3 wt. % Gr	13.82	-252	-147	105
Cu-30Zn + 0.5 wt. % Gr	5.50	-279	-151	128

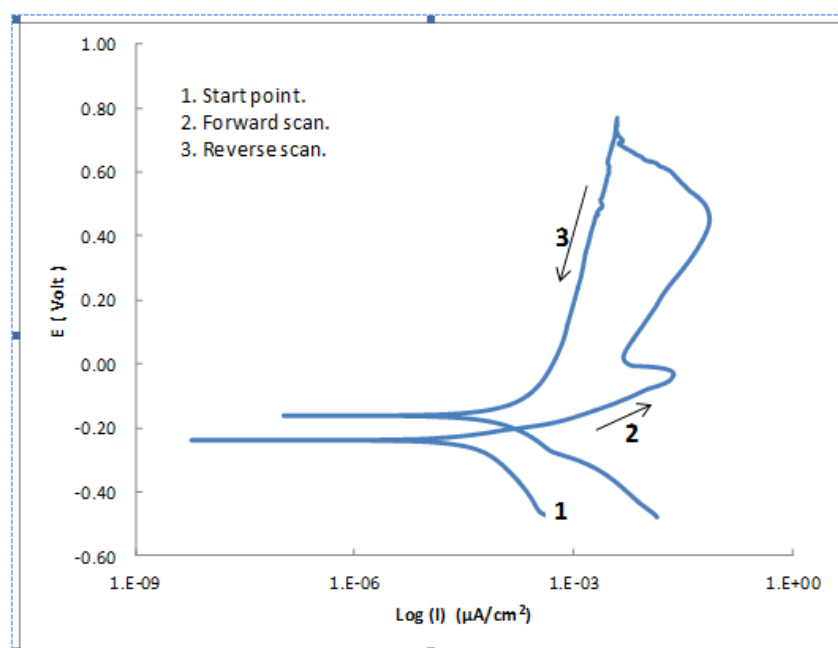


Figure 3. Potentiodynamic curve of Cu-30Zn.

3.2 Morfology

3.2.1 Prior Testing Morphology

Scanning electron microscope (SEM) was used to examine the morphological structure of surface of the base Cu-30Zn alloy prior to corrosion testing. SEM images shows the presence of scratches parallel to polishing and grinding lines as shown in Figure 4a. Also, several porosities were randomly distributed over the surface, as shown in Figure 4b. These porosities were probably formed during compaction process. Energy dispersive x-ray analysis (EDAX) spectrum of the intact surface contains only peaks of the alloy constituent elements, as shown in Figure 5.

For Cu-30Zn reinforced with graphite, scanning electron microscope image in Figure 6 shows the presence of ploughing grooves parallel to polishing lines at the surface (marked by A), smeared graphite clusters all over the surface (marked by B), and spalls with different depths and shapes (marked by C).

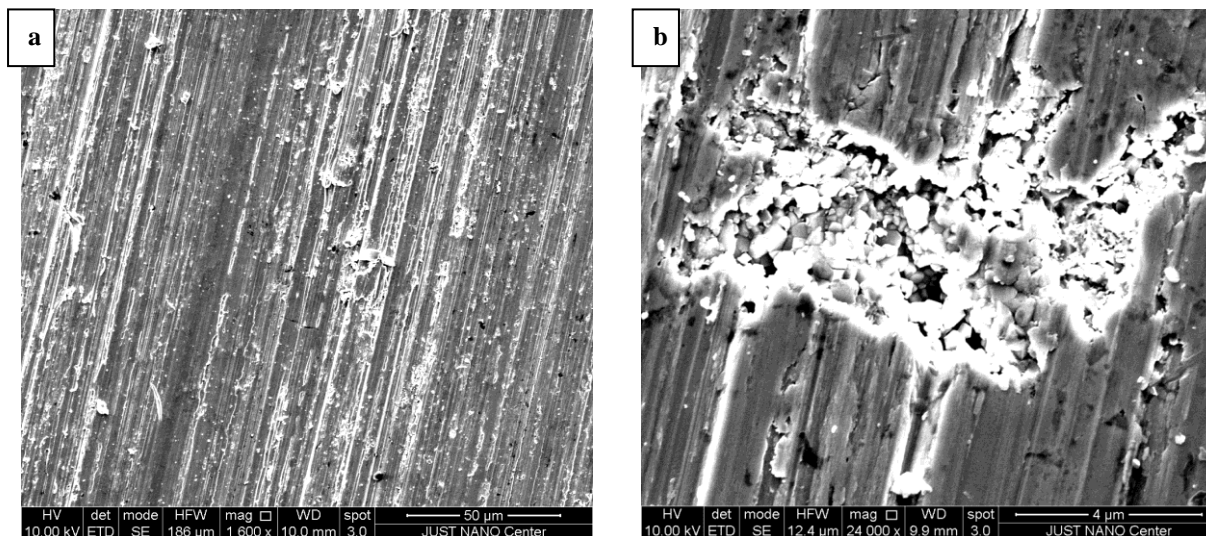


Figure 4. (a) SEM image of Cu-30Zn surface prior to corrosion testing. (b) A small porosity from imperfect compaction on Cu-30Zn surface.

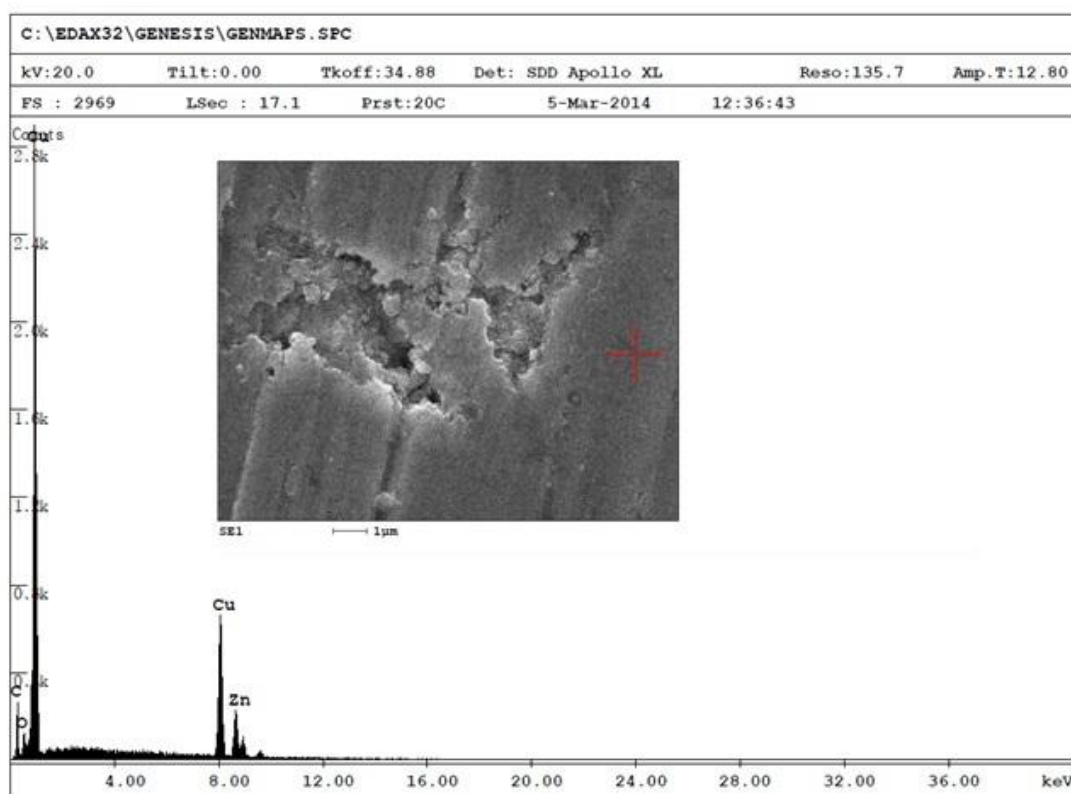


Figure 5. EDAX Spot analysis of the intact surface of Cu-30Zn alloy prior corrosion testing.

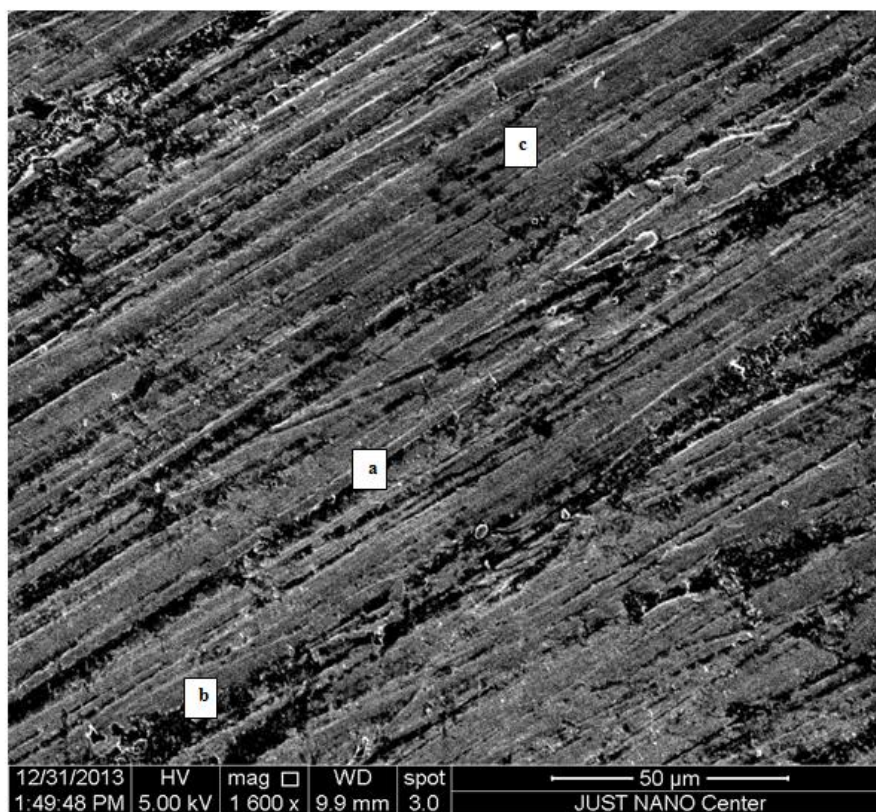


Figure 6. SEM image of the surface of Cu-30Zn reinforced with 0.5 wt% graphite prior corrosion testing.

3.2.2 Post Corrosion Morphology

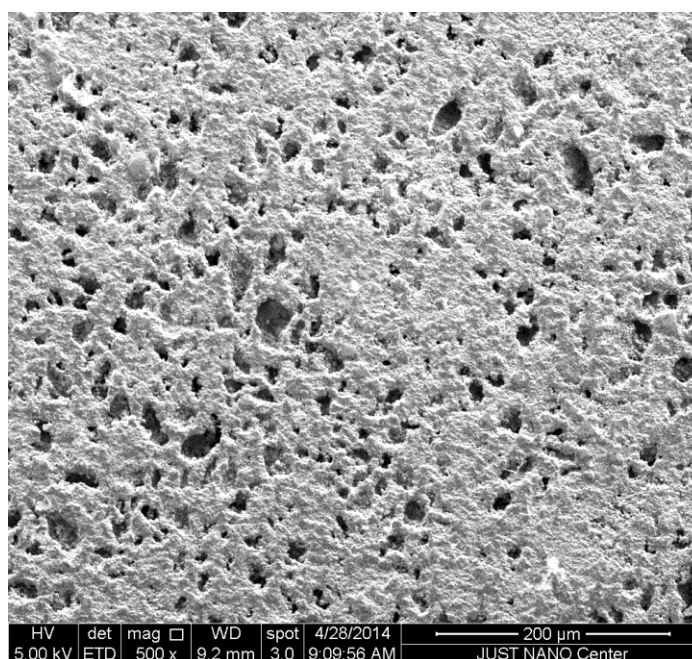


Figure 7. SEM image of the corroded surface of Cu-30Zn reinforced with graphite.

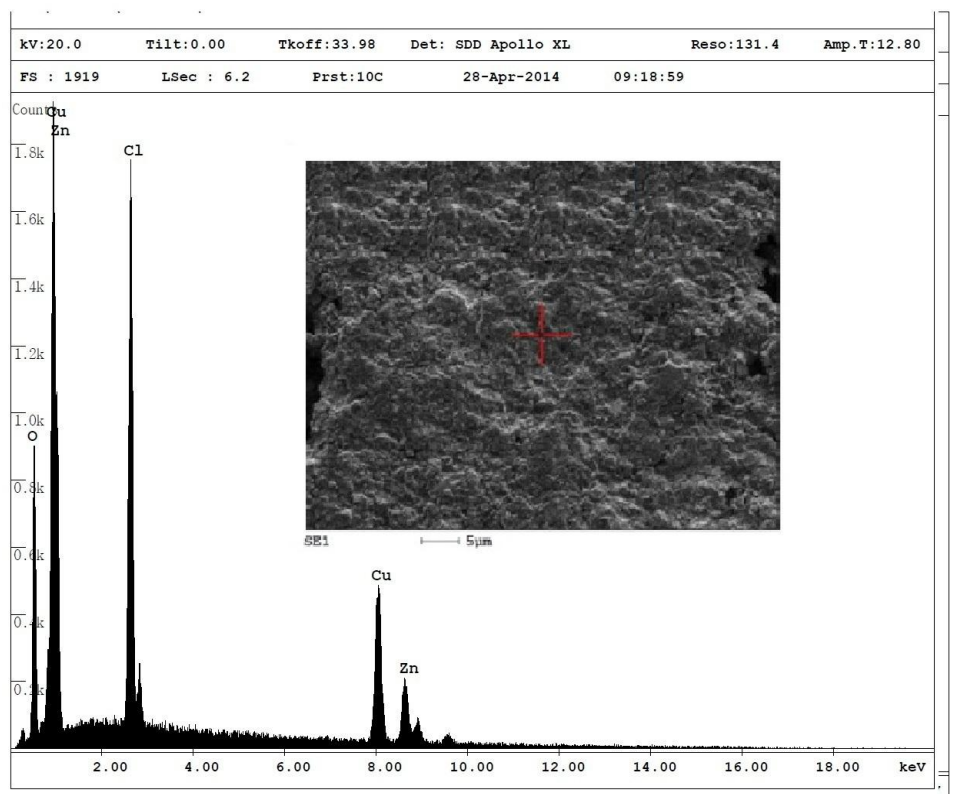


Figure 8. EDAX spectrum of Cu-30Zn reinforced with graphite surface after corrosion testing.

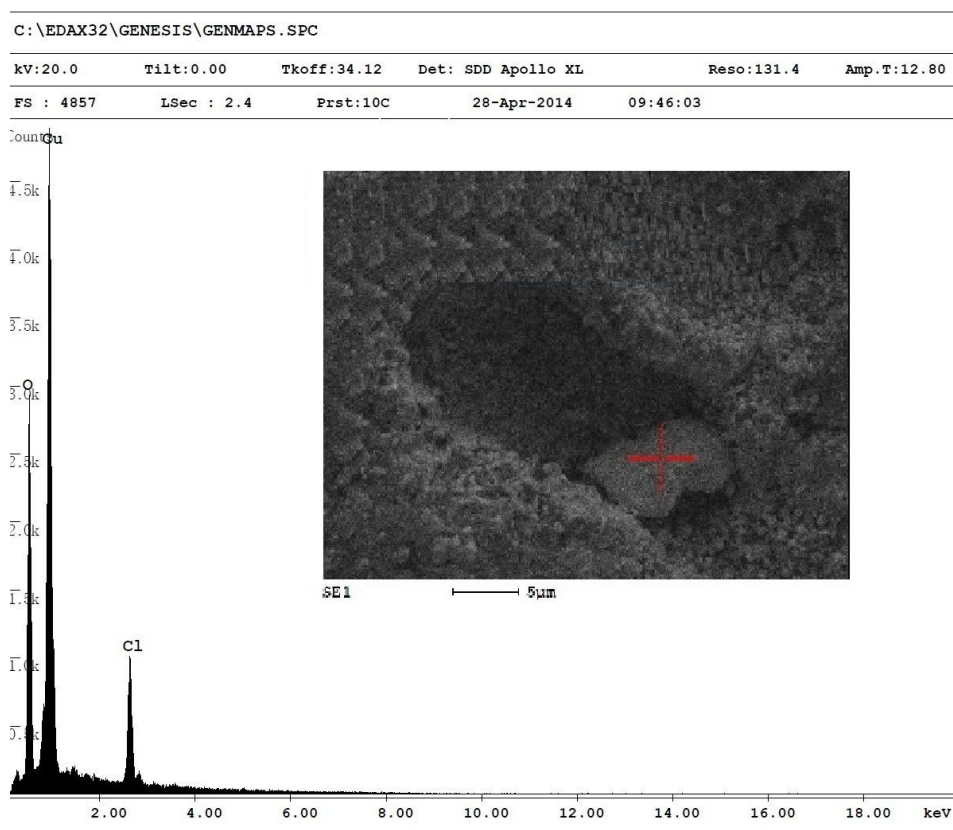


Figure 9. EDAX analysis of pit on the surface of Cu-30Zn reinforced with graphite.

The corroded surface of the composites reinforced with graphite has an interesting decorative appearance with large number of small shallow pits, as can be seen in Figure 7, where the bottom surface of the pits can be easily seen. This result is consistent with negative hysteresis obtained at electrochemical testing. Graphite peak was absent in the EDAX spectrum shown in Figure 8, the chlorine peak belongs to corrosion byproducts (metal chloride). Figure 9 shows an SEM image with EDAX spectrum of one of these pits. The pit has a large particle inside, and the spectrum indicates the presence of {Cu, O, Zn, and Cl} peaks at the particle indicating that this particle is more likely a corrosion product as CuCl_2 , CuO or Cu_2O .

4. CONCLUSIONS

The following conclusions can be drawn from the present work:

- Cu-30Zn reinforced with active graphite particles shows a higher tendency to uniform corrosion as compared to the corresponding monolithic matrix alloy. This behavior is primarily due to the formation of strong microgalvanic couple between matrix and conductive graphite reinforcing particles.
- The corrosion resistance of Cu-30Zn decreases with increase of graphite weight percentages due to the corresponding increase of cathodic area.
- The efficiency of corrosion product layer increased after transpassive dissolution stage. This is due to the formation of crevice regions at the particle matrix interface which impede propagation of pits into the matrix.
- The corroded surface of the composite is covered with the corrosion byproduct layer with large number of small shallow pits. This result is consistent with negative hysteresis attained at electrochemical testing.
- The use of graphite to reinforce Cu-30Zn must be addressed carefully with high level of awareness, and should be used in controlled weight fractions, as any extra amount of graphite will negatively impact on corrosion resistance of the composite.

ACKNOWLEDGEMENTS

This work was supported by a grant from the deanship of research at Jordan University of Science and Technology (J.U.S.T.) / (Grant No. 2013/ 78). The authors would like to thank all members of Engineering Workshop of J.U.S.T., J.U.S.T. Nanocenter, and Material Laboratory of Industrial Engineering Department for their help in completing this research work.

References

1. J. Singh and A. Chauhan, *Int. J. App. Eng. Res.*, 9 (2014)959.
2. U.S. Congress, Office of Technology Assessment, *Advanced Materials by Design*, OTA-E351 Washington, DC: U.S. Government Printing Office. 1988.
3. G.A. El-Mahdy, A.K.F. Dyab, A.M. Atta and H.A. Al-Lohedan, *Int. J. Electrochem. Sci.*, 8 (2013) 9858.

4. M.M. Antonijevic, G.D. Bogdanovic, M.B. Radovanoivc, M.B. Petrovic and A.T. Stamenkovic, *Int. J. Electrochem. Sci.*, 4 (2009) 654.
5. C. Vilarinho, J.P. Davim, D. Soares, F. Castro and J. Barbosa, *J. Mater. Process. Technol.*, 170 (2005) 441.
6. W. Ozgowicz, E.K. Ozgowics and B. Grzegorzcyk, *J. Achievements Mater. Manuf. Eng.*, 40 (2010) 15.
7. S. Tzamtzis, N.S. Barekar, N. Hari Babu, J. Patel, B.K. Dhnidaw and Z. Fan, *Composites: Part A.*, 40 (2009) 144.
8. R.S. Rana, R. Purohit and S. Das, *Int.J. Sci. Eng.Res.*, 3 (2012) 1.
9. S. Pournaderi, S. Mahdavi and F. Akhlaghi, *Powder Technol.*, 229 (2012) 276.
10. S.S. Yilmaz, B.S. Ünlü and R. Varol, *Mater. Des.*, 31 (2010) 4496.
11. S.F. Moustafa, Z. Abdel-Hamid and A.M. Abdel-Elhay, *Mater. Lett.*, 53 (2002) 224.
12. S. Li, H. Imai, H. Astumi and K. Kondoh, *Mater. Des.*, 32 (2011)192.
13. S. Li, H. Imai, K. Kondoh, A. Kojima, Y. Kosaka, K. Yamamoto and M. Takahashi, *Mater. Chem. Phys.*, 135 (2012) 644.
14. H. Astumi, H. Imai, S. Li, K. Kondoh, Y. Kousaka and A. Kojima, *Mater. Chem. Phys.*, 135 (2012) 554.
15. P.K. Rohatgi, D. Nath and A.N. Agrawal, *Corros. Sci.*, 42 (2000) 1553.
16. M.S. El-Sayed, A.A. Almajed, F. H. Latif and H. Junaedi, *Int. J. Electrochem. Sci.*, 6 (2011) 1085.
17. F.H. Latief, M.S. El-Sayed, A.A. Almajed and H. Junaedi, *J. Anal. Appl. Pyrolysis*, 92 (2011) 485.
18. M.A. Afifi, Internationally Scholarly Research Notices Corrosion. 2014, ID 279856.
19. J.E. Orth and H.G. Wheat, *Appl. Compos. Mater.*, 4 (1997) 305.
20. P.P. Trzaskoma, *Corrosion*, 42 (1986) 609.
21. L.H. Hihara and R.M. Latanision, *Corros. Sci.*, 34 (1993) 655.
22. G.A. El-Mahdy, *J. Appl. Electrochem.*, 35 (2005) 347.
23. I. Milošev and T. Kosec, *Chem. Biochem. Eng.*, 23 (2009) 53.
24. V.N. Gaitonde, S.R. Karnik and M.S. Jayaprakash, *J. Miner. Mater. Charact. Eng.*, 11 (2012) 659.
25. Yu-Mei Han and X.-Grant Chen, *Mater.*, 8 (2015) 6455.
26. F. El-Taib Heakal and Kh.A. Awad, *Int. J. Electrochem. Sci.*, 6 (2011) 6483.
27. M.A. Almomani and C.R. Aita, *J. Vac. Sci. Technol. A*, 27 (2009) 449.
28. S. Roepstorff and E. Maahn, Corrosion Resistance of Aluminum-Silicon Carbide Composite Materials. In Proceeding of the 12th Scandinavian Corrosion Congress and Eurocorr'92, Espoo, Finland, 31 May–4 June 1992.